

# Statistical evaporation of rotating clusters. II. Angular momentum distribution

P. Parneix

*Laboratoire de Photophysique Moléculaire, Bât. 210,  
Université Paris-Sud, F91405 Orsay Cedex, France*

F. Calvo

*Laboratoire de Physique Quantique, IRSAMC, Université Paul Sabatier,  
118 Route de Narbonne, F31062 Toulouse Cedex, France*

The change in the angular momentum of an atomic cluster following evaporation is investigated using rigorous phase space theory and molecular dynamics simulations, with an aim at the possible rotational cooling and heating effects. Influences of the shape of the interaction potential, anharmonicity of the vibrational density of states (DOS), and the initial distribution of excitation energies are systematically studied on the example of the Lennard-Jones cluster LJ<sub>14</sub>. For this system, the predictions of PST are in quantitative agreement with the results of the simulations, provided that the correct forms for the vibrational density of states and the interaction potential are used. The harmonic approximation to the DOS is used to obtain explicit forms for the angular momentum distribution in larger clusters. These are seen to undergo preferential cooling when thermally excited, and preferential heating when subject to a strong vibrational excitation.

## I. INTRODUCTION

When a polyatomic system is vibrationally excited, it may undergo spontaneous dissociation on a suitable time scale. Most often, different dissociation channels are available, which may or may not be selected upon energetic criteria only. Rotational excitations are also very important, because they directly influence the relative amount of kinetic energy released in translational modes. Kinetic energies released are of constant use in experiments for extracting information about binding energies, temperatures, and more generally nanocalorimetry data (see Refs. 1,2,3 and references therein).

Rotational excitations practically act in two distinct ways. The first is direct, and reflects the greater ease of fragmenting the system due to centrifugal forces. The second way is indirect, and lies in the coupling between vibrational and rotational motion: because the system is not rigid, it may rearrange so as to reduce its angular velocity, thereby enhancing its stability. When an isolated cluster dissociates into two fragments, the angular momentum  $\vec{J}$  is splitted into two parts, namely the orbital momentum  $\vec{L}$  of the fragments in their relative motion, and the remaining angular momentum  $\vec{J}_r$  associated with the fragments themselves. It is very easy to see that, at low initial value of  $\vec{J}$ ,  $\vec{L}$  nearly compensates  $\vec{J}_r$ . Hence, for a large system emitting a single atom, rotational heating is expected at low  $J$ . On the opposite, rapidly rotating clusters are more likely to lose angular momentum following evaporation, a phenomenon known as rotational cooling. These aspects of fragmentation have been previously investigated by Stace,<sup>4</sup> who used simple statistical models to emphasize the role of rotational temperature in the interpretation of experiments.

In our previous work,<sup>5</sup> we performed molecular dynamics (MD) simulations as well as theoretical calculations based on the phase space theory (PST) to extract the distributions of kinetic energies released upon evaporation in small Lennard-Jones (LJ) atomic clusters. Our main result was to show that PST could be quantitatively accurate in a broad range of total energies and angular momenta, provided that the vibrational and rotational densities of states, as well as the interaction potential between the fragments, were all correctly accounted for. This result was previously proved by Weerasinghe and Amar for nonrotating clusters,<sup>6</sup> and partially observed for aluminium clusters by Peslherbe and Hase,<sup>7,8</sup> though these authors used a simple  $C/r^n$  form for the dissociation potential, which induced some deviations between theory and simulation at large excitations.

Here we will focus on angular momentum properties, namely their distributions and mean values, and how they are affected by the initial excitation. The present approach follows our previous effort,<sup>5</sup> with the same aim at assessing phase space theory in a quantitative comparison with simulations. In the next section, we briefly recall the main equations underlying the PST calculation of the angular momentum properties of the product cluster, and we treat separately the simple cases of an harmonic vibrational density of states, an interaction potential with the form  $C/r^n$ , or an initially nonrotating cluster. Our application to small and medium size Lennard-Jones clusters for various types of excitations is treated in Sec. III. In Sec. IV we discuss our results with respect to the works by Stace<sup>4</sup> and those by Peslherbe and Hase,<sup>8</sup> before finally concluding.

## II. PHASE SPACE THEORY

In this Section, we give the main expressions for the angular momentum distribution of the product cluster following evaporation. To obtain such information, conservation of total angular momentum and energy has to be included, which is the case in the phase space theory developed by Pechukas and Light,<sup>9,10</sup> Klots,<sup>11,12</sup> and Chesnavich and Bowers.<sup>13,14,15</sup>

Here we consider a parent cluster characterized by a rotational angular momentum  $J$  and a total rovibrational energy  $E$ . We denote by  $J_r$  the rotational angular momentum of the product cluster after dissociation. The unnormalized probability of finding a dissociation event characterized by the angular momentum  $J_r$  of the product cluster within  $dJ_r$  and the energy released  $\varepsilon_{\text{tr}}$  within  $d\varepsilon_{\text{tr}}$  can be written as<sup>14</sup>

$$\mathcal{P}(\varepsilon_{\text{tr}}, J_r; E, J) = \Omega_n^{(J_r)}(E - E_0 - \varepsilon_{\text{tr}}) \int_{L_{\min}(\varepsilon_{\text{tr}}, J_r)}^{L_{\max}(\varepsilon_{\text{tr}}, J_r)} \Gamma(\varepsilon_r^*, J_r) dL. \quad (1)$$

In this equation,  $\Omega_n^{(J_r)}$  is the vibrational density of states of the product cluster having angular momentum  $J_r$ ,  $\Gamma(\varepsilon_r^*, J_r)$  is the available volume of states with rotational energy lower than  $\varepsilon_r^*$  in angular momentum space. For a given  $\varepsilon_{\text{tr}}$ , the rotational density of states is given by the sum of this quantity over the accessible area in the  $(J_r, L)$  plane, with  $L$  the orbital angular momentum. This area is limited by mechanical (angular momentum and energetic) constraints, and will be discussed below. If both  $\varepsilon_{\text{tr}}$  and  $J_r$  are fixed, the integration must be performed in a range of  $L$  limited by  $L_{\min}$  and  $L_{\max}$ . In this paper, we are interested in the distribution of angular momentum of the product cluster. The probability of finding a particular value of  $J_r$  within  $dJ_r$  is simply the integral of  $\mathcal{P}$  over all possible values of  $\varepsilon_{\text{tr}}$ :

$$P(J_r; E, J) = \int_{\varepsilon_{\text{tr}}^{\min}}^{E-E_0} \mathcal{P}(\varepsilon_{\text{tr}}, J_r; E, J) d\varepsilon_{\text{tr}} \quad (2)$$

In PST the products are located at the transition state. Here we will consider rather large clusters, and our main assumption will be to treat the evaporative system  $\text{LJ}_{n+1} \rightarrow \text{LJ}_n + \text{LJ}$  within the sphere+atom model. In this case, the available volume  $\Gamma(\varepsilon_r^*, J_r)$  is simply given by  $2J_r$ .<sup>20</sup> Therefore the probability of finding a dissociation event with angular momentum  $J_r$ , starting from a total energy  $E$  and a total angular momentum  $J$  is given by:

$$P(J_r; E, J) = P_0 \times 2J_r \int_{\varepsilon_{\text{tr}}^{\min}}^{E-E_0} \Omega_n^{(J_r)}(E - E_0 - \varepsilon_{\text{tr}}) [L_{\max}(\varepsilon_{\text{tr}}, J_r) - L_{\min}(\varepsilon_{\text{tr}}, J_r)] d\varepsilon_{\text{tr}}, \quad (3)$$

where the normalization constant  $P_0$  accounts for channel and rotational degeneracies, and also depends on the parent density of states  $\Omega_{n+1}^{(J)}(E)$ . In the following, we will make use of the notation  $\Delta L(\varepsilon_{\text{tr}}, J_r) = L_{\max}(\varepsilon_{\text{tr}}, J_r) - L_{\min}(\varepsilon_{\text{tr}}, J_r)$ . The problem is now reduced to determining  $\Delta L(\varepsilon_{\text{tr}}, J_r)$ .

We first consider the case of a radial dissociation potential  $V(r)$  given by  $V(r) = -C_n/r^p$ , with  $p > 2$ . Since the kinetic energy must be positive at the centrifugal barrier, the well known energetic constraint can be easily found:

$$B_n J_r^2 + L^{2p/(p-2)}/\Lambda_p \leq \varepsilon_{\text{tr}}, \quad (4)$$

where we have introduced the rotational constant  $B_n$  of the product cluster  $\text{LJ}_n$ , and the Langevin parameter  $\Lambda_p$  given as a function of  $p$ ,  $C_n$ ,  $\hbar$  and the reduced mass  $\mu_n$  by

$$\Lambda_p = \frac{2}{p-2} C_n^{2/(p-2)} \left( \frac{\mu_n p}{\hbar^2} \right)^{p/(p-2)}. \quad (5)$$

The second boundary comes from the conservation of angular momentum,  $\vec{J} = \vec{J}_r + \vec{L}$ , or more conveniently:

$$|J_r - L| \leq J \leq J_r + L. \quad (6)$$

Let us denote by  $\mathcal{C}$  the set of  $(J_r, L)$  points that fulfill the equation  $\varepsilon_{\text{tr}} = L^{2p/(p-2)}/\Lambda_p + B_n J_r^2$ . For a given value of  $J_r$ , we define  $\varepsilon_{\text{tr}}^{\min}$  (resp.  $\varepsilon_{\text{tr}}^{\text{int}}$ ) as the values of  $\varepsilon_{\text{tr}}$ , which correspond to the intersection between  $\mathcal{C}$  and  $L = |J - J_r|$  (resp.  $L = J + J_r$ ). We find

$$\varepsilon_{\text{tr}}^{\min} = B_n J_r^2 + \frac{|J - J_r|^{2p/(p-2)}}{\Lambda_p} \quad \text{and} \quad \varepsilon_{\text{tr}}^{\text{int}} = B_n J_r^2 + \frac{(J + J_r)^{2p/(p-2)}}{\Lambda_p} \quad (7)$$

Obviously,  $\varepsilon_{\text{tr}}^{\text{min}}$  and  $\varepsilon_{\text{tr}}^{\text{int}}$  can not be larger than the maximum available energy  $E - E_0$ , and the largest value for  $J_r$  will be reached when  $\varepsilon_{\text{tr}}^{\text{min}} = E - E_0$ . In Fig. 1, a simple scheme summarizes the integration procedure in the  $(J_r, L)$  plane. In this figure,  $\mathcal{C}_{\text{min}}$  and  $\mathcal{C}_{\text{int}}$  are the contours  $\mathcal{C}$  for  $\varepsilon_{\text{tr}} = \varepsilon_{\text{tr}}^{\text{min}}$  and  $\varepsilon_{\text{tr}} = \varepsilon_{\text{tr}}^{\text{int}}$ , respectively. When  $\varepsilon_{\text{tr}}^{\text{min}} \leq \varepsilon_{\text{tr}} \leq \varepsilon_{\text{tr}}^{\text{int}}$ ,  $\Delta L(\varepsilon_{\text{tr}}, J_r)$  is given by  $\mathcal{L}(\varepsilon_{\text{tr}}, J_r) - |J - J_r|$ , where  $\mathcal{L}(\varepsilon_{\text{tr}}, J_r) = [\Lambda_p(\varepsilon_{\text{tr}} - B_n J_r^2)]^{(p-2)/2p}$ . On the other hand, when  $\varepsilon_{\text{tr}}^{\text{int}} \leq \varepsilon_{\text{tr}} \leq E - E_0$ ,  $\Delta L(\varepsilon_{\text{tr}}, J_r) = (J + J_r) - |J - J_r|$ .

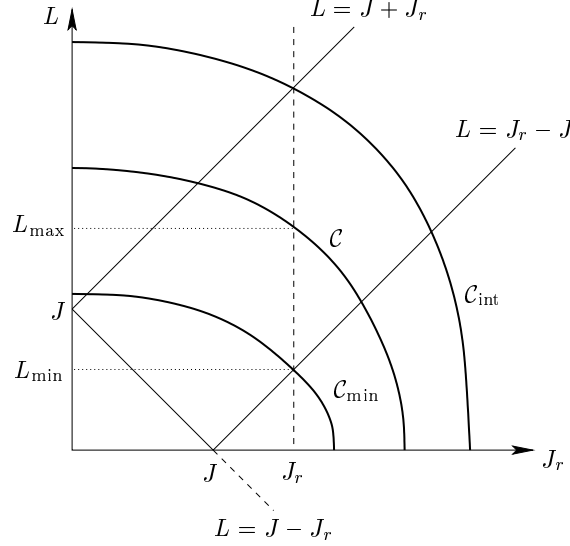


FIG. 1: Schematic representation of the  $(J_r, L)$  integration plane.

One interesting case is the harmonic limit of this model. For this we consider the harmonic VDOS for the product cluster,  $\Omega_n(E) \propto E^{s-1}$  with  $s = 3n - 6$ . After replacing the expressions for  $\Delta L(\varepsilon_{\text{tr}}, J_r)$  obtained above, equation (3) now becomes

$$\begin{aligned}
 P_h(J_r; E, J) &\propto 2J_r \int_{\varepsilon_{\text{tr}}^{\text{min}}}^{\varepsilon_{\text{tr}}^{\text{int}}} (E - E_0 - \varepsilon_{\text{tr}})^{s-1} \mathcal{L}(\varepsilon_{\text{tr}}, J_r) d\varepsilon_{\text{tr}} \\
 &\quad - 2J_r |J - J_r| \int_{\varepsilon_{\text{tr}}^{\text{min}}}^{\varepsilon_{\text{tr}}^{\text{int}}} (E - E_0 - \varepsilon_{\text{tr}})^{s-1} d\varepsilon_{\text{tr}} \\
 &\quad + 2J_r (J + J_r - |J - J_r|) \int_{\varepsilon_{\text{tr}}^{\text{int}}}^{E-E_0} (E - E_0 - \varepsilon_{\text{tr}})^{s-1} d\varepsilon_{\text{tr}},
 \end{aligned} \tag{8}$$

By considering the analytical expression for  $\mathcal{L}(\varepsilon_{\text{tr}}, J_r)$  given previously and using the notation  $\gamma = (p-2)/2p$ , we thus obtain

$$\begin{aligned}
 P_h(J_r; E, J) &\propto 2J_r \Lambda_p^\gamma \int_{\varepsilon_{\text{tr}}^{\text{min}}}^{\varepsilon_{\text{tr}}^{\text{int}}} (E - E_0 - \varepsilon_{\text{tr}})^{s-1} (\varepsilon_{\text{tr}} - B_n J_r^2)^\gamma d\varepsilon_{\text{tr}} \\
 &\quad - \frac{2J_r |J - J_r|}{s} [(E - E_0 - \varepsilon_{\text{tr}})^s]_{\varepsilon_{\text{tr}}^{\text{min}}}^{\varepsilon_{\text{tr}}^{\text{int}}} \\
 &\quad + \frac{2J_r (J + J_r - |J - J_r|)}{s} [(E - E_0 - \varepsilon_{\text{tr}})^s]_{E-E_0}^{\varepsilon_{\text{tr}}^{\text{int}}}.
 \end{aligned} \tag{9}$$

This equation can be further simplified into

$$\begin{aligned}
 P_h(J_r; E, J) &\propto \frac{2J_r (J + J_r)}{s} (E - E_0 - \varepsilon_{\text{tr}}^{\text{int}})^s \\
 &\quad - \frac{2J_r |J - J_r|}{s} (E - E_0 - \varepsilon_{\text{tr}}^{\text{min}})^s + 2J_r \Lambda_p^\gamma \mathcal{I}_{s, \gamma},
 \end{aligned} \tag{10}$$

where  $\mathcal{I}_{s,\gamma}$  is short for the integral in Eq. (9). This integral can be written explicitly as

$$\mathcal{I}_{s,\gamma} = \sum_{k=0}^{s-1} \binom{s-1}{k} \frac{(-1)^{s-1-k}}{s-k+\gamma} \frac{(E-E_0-B_n J_r^2)^k}{\Lambda_p^{s-k+\gamma}} \left[ (J+J_r)^{1+(s-k)/\gamma} - |J-J_r|^{1+(s-k)/\gamma} \right]. \quad (11)$$

All the formalism above has been derived by assuming an interaction potential with the form  $V(r) = -C_n/r^p$ . As discussed in our previous work,<sup>5</sup> this expression does not give a very good account of the finite extension of the cluster, and a better representation of the atom-cluster interaction is provided by  $V(r) = -C_n/(r-r_0)^p$ , with  $r_0 > 0$ . In this case, and more generally for an arbitrary form of  $V(r)$ , the computation of  $L_{\min}(\varepsilon_{\text{tr}}, J_r)$  and  $L_{\max}(\varepsilon_{\text{tr}}, J_r)$  must be carried out numerically. For a series of  $L$ , the location  $r^*(L)$  and the height  $\varepsilon^\dagger(L)$  of the centrifugal barrier is obtained. At a given  $\varepsilon_{\text{tr}}$ , the integration boundaries become

$$\begin{cases} \varepsilon^\dagger(L) + B_n J_r^2 \leq \varepsilon_{\text{tr}}, \\ |J_r - L| \leq J \leq J_r + L \end{cases} \quad (12)$$

and the limits  $L_{\min}(\varepsilon_{\text{tr}}, J_r)$  and  $L_{\max}(\varepsilon_{\text{tr}}, J_r)$  can thus be directly calculated from the knowledge of  $\varepsilon^\dagger(L)$ .

When we do not specify the harmonic limit to extract  $P(J_r; E, J)$ , equation (3) is used with the anharmonic vibrational densities of states  $\Omega^{(J_r)}(E)$ , which includes some dependency with  $J_r$ . To calculate  $\Omega^{(J_r)}(E)$ , we have used the Monte Carlo method proposed in Ref. 19, further improved with the parallel tempering accelerating scheme.<sup>21</sup> The multiple histogram method<sup>22</sup> was then used to estimate the configurational densities of states and, through a simple convolution product, the total VDOS. In practice, we have neglected the variations of  $\Omega$  with  $J_r$ , and used the approximation  $J_r \approx J$ . As will be seen below, this does not entail a significant error.

The dissociation potential  $V(r)$  felt by an atom leaving the  $n$ -atom LJ cluster was taken from our previous work,<sup>5</sup> and approximated by the form  $-C_6/(r-r_0)^6$  form. The coefficients  $C_6$  and  $r_0$  have been deduced from a fitting of constrained Monte Carlo simulations at finite temperature, as well as some Wang-Landau simulations. Their values are given in Ref. 5.

For each value of angular momentum, we have also carried out one or several sets of 5000 independent molecular dynamics trajectories, used as reference data. The angular momentum distribution has been calculated for different values of the initial total angular momentum between  $J = 0$  and  $J \approx 5$  LJ units.<sup>23</sup> For the details of the MD simulations, we also refer the reader to Ref. 5.

### III. RESULTS

The energetics of unimolecular evaporation has been considered in our previous article,<sup>5</sup> and we only focus here on the angular momentum distribution following the evaporation of a rotating atomic cluster. In the form detailed above, phase space theory directly gives us access to this distribution. The sharing between rotational energy of the product cluster and the translational kinetic energy released can then be analysed.

We first consider the unimolecular dissociation involving the nearly spherical LJ<sub>13</sub> product cluster. The reaction studied here is thus LJ<sub>14</sub>  $\rightarrow$  LJ<sub>13</sub>+LJ. In Fig. 2 we have plotted the angular momentum distribution of the LJ<sub>13</sub> product cluster, as estimated from PST. The rotational constant  $B$  of LJ<sub>13</sub> was taken at  $T = 0.3$ , such that  $B = 0.0444$  LJ units.<sup>5</sup> Two values of the initial angular momentum, namely  $J = 0.5$  and  $J = 3$ , were considered and the initial rovibrational energy was taken equal to  $E = -29$  LJ units in both cases. Different approximations were assessed and a good overall agreement with MD results is obtained. In Fig. 2(a), two different interaction potentials were selected along with the anharmonic density of states for both calculations. The interaction potential corresponding to  $T = 0.3$  is computed from MC simulations, and the  $r_0 = 0$  approximation refers to the long-range part of the exact LJ potential, with  $C_6 = 4n$  units. As can be seen from Fig. 2(a), the  $r_0 = 0$  approximation performs slightly less than the numerically exact radial potential, but still allows to reproduce quite accurately the MD results. The  $r_0 = 0$  approximation tends to underestimate the angular momentum of the product cluster, a feature previously noticed by Peshlherbe and Hase.<sup>8</sup> In Fig. 2(b), the harmonic limit has been tested for  $J = 3$ . Even though a very good agreement is obtained when considering the anharmonic DOS, some discrepancy with MD becomes to appear in the harmonic case. A change in slope has to be noted at  $J_r = J$  in Figs. 2(a) and especially 2(b). This discontinuity in the derivative of  $P(J_r; E, J)$  is due to the modulus  $|J_r - J|$  term in the definition of  $\varepsilon_{\text{tr}}^{\min}$ . Taking the derivative of Eq. 3 as a function of  $J_r$  actually leads to the following value for the change in slope across  $J = J_r$ :

$$\begin{aligned} \Delta \left( \frac{\partial P}{\partial J_r} \right) &= \left. \frac{\partial P}{\partial J_r} \right|_{J=J_r^+} - \left. \frac{\partial P}{\partial J_r} \right|_{J=J_r^-} \\ &= -4P_0 J \int_{B_n J^2}^{E-E_0} \Omega_n^{(J)}(E-E_0-\varepsilon_{\text{tr}}) d\varepsilon_{\text{tr}}. \end{aligned} \quad (13)$$

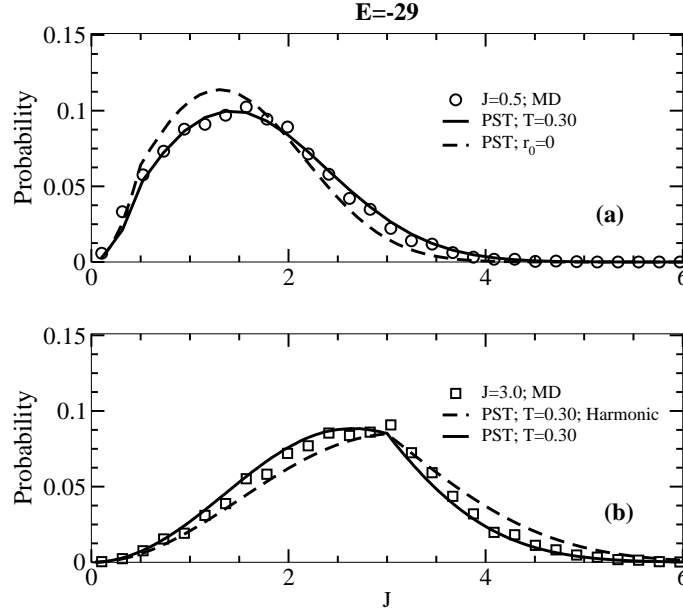


FIG. 2: Angular momentum distribution of  $J_r$  for the reaction  $\text{LJ}_{14} \rightarrow \text{LJ}_{13} + \text{LJ}$  at  $E = -29$ , for two different values of the initial angular momentum  $J$ . (a)  $J = 0.5$ ; (b)  $J = 3$ .

Therefore the slope necessary decreases at  $J_r = J$ , independently of the dissociation potential. In order to put this effect into evidence, we have run 15 sets of 5000 trajectories at  $J = 3.0$  [see Fig. 2(b)]. Within this statistics, a change in the slope around  $J_r = J$  can be effectively characterized, as seen in the statistical PST formalism.

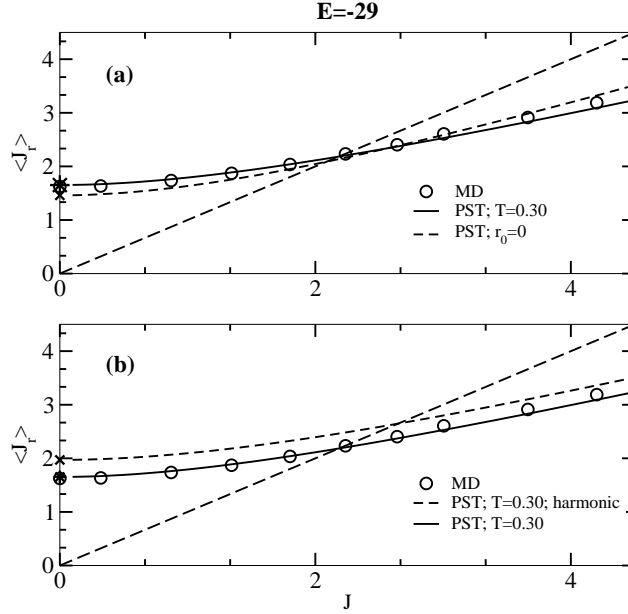


FIG. 3:  $\langle J_r \rangle$  versus  $J$  for the reaction  $\text{LJ}_{14} \rightarrow \text{LJ}_{13} + \text{LJ}$  at  $E = -29$  within different approximations: (a) effect of the radial potential; (b) effect of the anharmonicity of the PES. The  $J = 0$  values, obtained from Eq. (14), are represented by stars or crosses.

In Fig. 3, the mean angular momentum of the product cluster  $\langle J_r \rangle$  has been plotted as a function of  $J$  at the rovibrational energy  $E = -29$ . The same assumptions as in the previous figure have been tested. The line  $\langle J_r \rangle = J$  has also been shown in order to visualize more easily the rotational cooling or heating effects. First of all it is striking that the statistical PST model allows to perfectly reproduce the MD results when both the anharmonic DOS and the numerically exact radial potential are considered. The  $r_0 = 0$  approximation tends to underestimate  $\langle J_r \rangle$  in the low

$J$  regime. As  $J$  goes to 0, one recovers the exact limit of Eq. (3) given by

$$P(J_r; E, J = 0) = P_0 \times 2J_r \int_{B_n J_r^2 + \varepsilon^\dagger(J_r)}^{E - E_0} \Omega_n^{(J_r)}(E - E_0 - \varepsilon_{\text{tr}}) d\varepsilon_{\text{tr}}. \quad (14)$$

The harmonic approximation to this equation is straightforward:

$$P(J_r; E, J = 0) \propto J_r [E - E_0 - B_n J_r^2 - \varepsilon^\dagger(J_r)]^s. \quad (15)$$

On the contrary, in the high  $J$  limit,  $\langle J_r \rangle$  is overestimated. As  $J$  increases, the orbital transition state reaches small values, which explains that the  $r_0 = 0$  radial potential does not allow a correct description of the dissociation process. On the other hand the harmonic limit tends to underestimate  $\langle J_r \rangle$  on the whole domain of  $J$  considered in this study. Therefore the harmonic model with  $r_0 = 0$  could well give results in quantitative agreement with MD in the low  $J$  regime, but this would remain fortuitous.

Let  $J_c$  be the value of the initial angular momentum for which  $\langle J_r \rangle = J$ . For  $J < J_c$ , evaporation leads to an increase in the mean angular momentum, the so-called rotational heating process. High initial values of  $J$  more likely result in a decrease of angular momentum corresponding to rotational cooling. At  $E = -29$  LJ units,  $J_c$  turns out to be approximately equal to 2.2 units. As seen from the previous figures,  $J_c$  weakly depends on the dissociation potential, but is more sensitive to the harmonic approximation to the vibrational density of states.

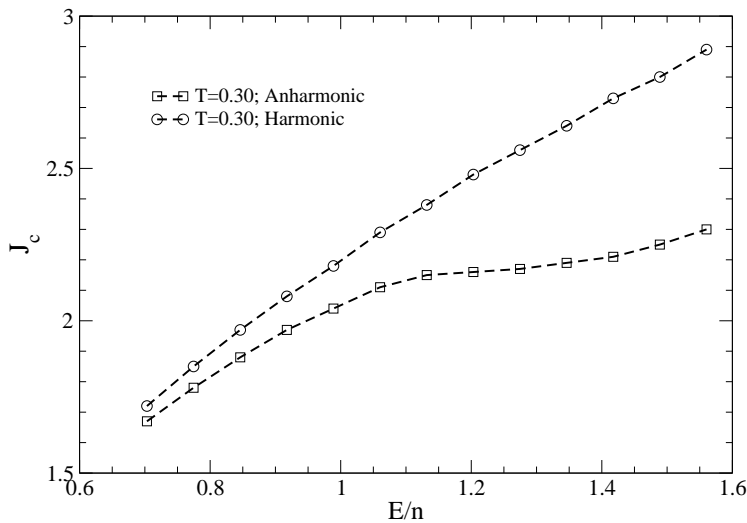


FIG. 4:  $J_c$  as a function of  $E/n$  for the reaction  $\text{LJ}_{14} \rightarrow \text{LJ}_{13} + \text{LJ}$ .

In Fig. 4 we follow the evolution of  $J_c$  as a function of the internal energy per atom  $E/n$ .  $J_c$  was calculated with the numerically exact radial potential, both in the harmonic and anharmonic approximations to the VDOS. In the low energy regime, the cluster tends to be harmonic and both approximations give similar results. At higher energies, especially close to the melting phase change of  $\text{LJ}_{13}$  and beyond, stronger differences appear. Between  $E/n = 1.1$  and  $E/n = 1.4$ ,  $J_c$  reaches a plateau similar to the plateau in the microcanonical temperature at the same energy, but only within the anharmonic description. The same plateau must also be correlated with the one in the average kinetic energy released, as seen in Refs. 5,6, and 17. Hence, large internal energies in the parent cluster indeed requires an anharmonic treatment of vibration to extract quantitative informations about the threshold between rotational cooling and heating effects.

Up to now we have only analyzed product angular momentum distributions for a given initial angular momentum  $J$  and an internal rovibrational energy  $E$ . We will now consider physically realistic conditions, where both internal energy and angular momentum are drawn from thermal distributions. The initial angular momentum distribution  $f(J)$  for the spherical cluster  $\text{LJ}_{n+1}$  is given by  $f(J) \propto J^2 \exp(-B_{n+1} J^2 / k_B T_{\text{rot}})$ . The distribution of the initial vibrational energy  $f(E)$  follows the VDOS, and we have allowed for a possible extra amount of energy  $\Delta E$  brought by a specific excitation process (collision, photoexcitation, ionization,...). Therefore  $f(E) \propto \Omega_{n+1}^{(J)}(E - \Delta E) \exp[-(E - \Delta E)/k_B T_{\text{vib}}]$ . The

distribution of product angular momentum then reads

$$P(J_r) \propto \iint J^2 \Omega_{n+1}(E - \Delta E) \exp \left[ -\frac{E - \Delta E}{k_B T_{\text{vib}}} - \frac{B_{n+1} J^2}{k_B T_{\text{rot}}} \right] P(J_r; E, J) dJ dE \quad (16)$$

The initial vibrational and rotational temperatures may be different, because the extra energy  $\Delta E$  is converted into vibrational energy. In Fig. 5 two physical situations have thus been studied. The first one corresponds to a parent

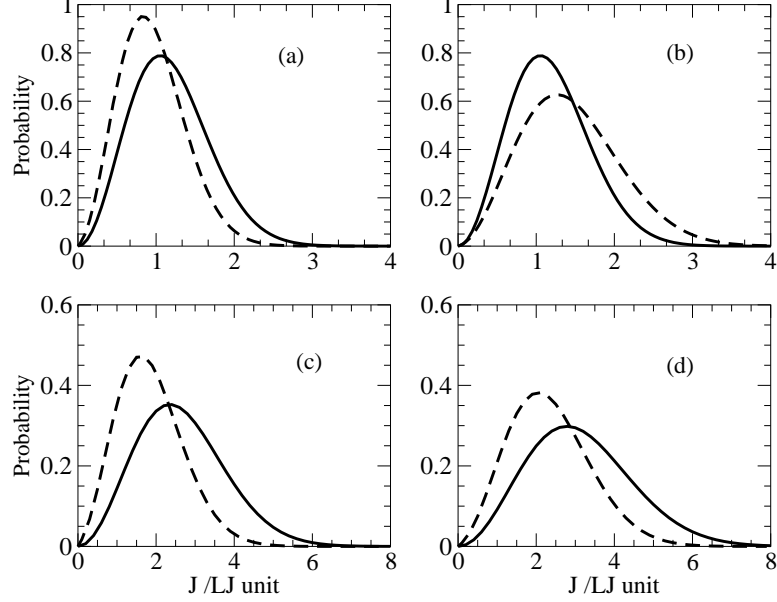


FIG. 5: Initial and final angular momenta following the evaporation of  $\text{LJ}_{14}$  for different physical conditions characterized by their thermal distributions and the extra excitation energy. (a)  $T = 0.05$  and  $\Delta E = 5$ ; (b)  $T = 0.05$  and  $\Delta E = 8$ ; (c)  $T = 0.20$  and  $\Delta E = 0$ ; (d)  $T = 0.40$  and  $\Delta E = 0$ .

cluster prepared at low temperature ( $T = 0.05$ ), for which two possible values of  $\Delta E$  have been added, namely either  $\Delta E = 4$  or  $\Delta E = 8$  LJ units. This situation is typical of a cluster prepared in a supersonic expansion and photoexcited in the infrared domain. In Fig. 5(a), the final distribution of  $J$  is slightly shifted to lower values. This is indicative of rotational cooling. In this case, the mean  $E/n$  is almost equal to 0.4. An extrapolation from Fig. 4 shows that  $J_c$  will be approximately equal to 0.9, a value that is smaller than the initial angular momentum. It explains why cooling occurs under these physical conditions. On the other hand, in Fig. 5(b),  $E/n \approx 0.7$  and  $J_c$  is increased to about 1.7. This value is larger than the mean value of the initial angular momentum, which is consistent with the observed rotational heating.

We have also simulated a pure thermal excitation of the cluster at a temperature large enough to induce dissociation on a reasonable time scale, that is accessible to MD. Therefore the thermal distributions are directly considered for  $E$  and  $J$  with  $\Delta E = 0$ , and  $T_{\text{rot}} = T_{\text{vib}}$ . We have considered two different temperatures,  $T = 0.2$  and  $0.4$ , and in both cases rotational cooling appears as the direct consequence of  $\langle J \rangle > J_c$ . The efficiency of the cooling process can be analysed by adjusting the product angular momentum distribution to a Boltzmann law. For example, the thermalized cluster initially at  $T^{(i)} = 0.4$  used in Fig. 5(d) yields a final rotational temperature close to  $T^{(f)} = 0.16$ . At this initial temperature,  $E/n$  is approximately 1, and from Fig. 4 we see that the harmonic approximation would significantly underestimate rotational cooling.

Finally we have investigated larger clusters, within the harmonic approximation as well as the simplest case for the radial potential, given by  $r_0 = 0$  and  $C_6 = 4n$  LJ units. The rotational constant  $B_n$  has been taken proportional to  $n^{-5/3}$ , with the proportionality factor calculated from the  $\text{LJ}_{13}$  cluster at  $T = 0$ . The value of  $E_0$ , the energy difference between  $\text{LJ}_{n+1}$  and  $\text{LJ}_n$ , has been taken to 6.4 for all sizes, a good approximation in the present size range of interest.

In Fig. 6 the angular momentum distribution before (solid line) and after (dashed line) evaporation is shown for  $n = 50$  and  $n = 100$  with an initial (vibrational and rotational) temperature  $T = 0.5$ . The adjustment to a thermal distribution is also shown. At this initial temperature, the final rotational temperature is equal to 0.36. It has to be noted that the final distribution is slightly non-Boltzmann (more peaked) with respect to the adjusted thermal distribution. Within the present harmonic approximation, it is found that the extent of rotational cooling does not

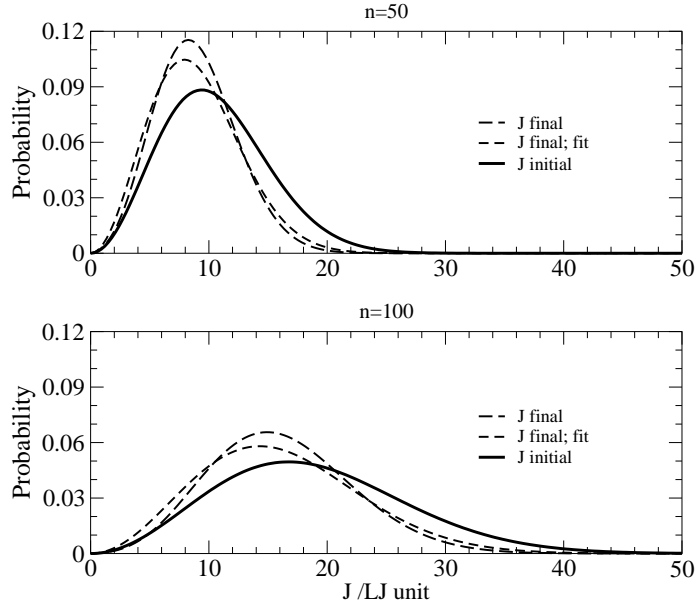


FIG. 6: Distribution of initial and final angular momenta from thermal excitations of  $\text{LJ}_{n+1}$  at  $T = 0.5$ . The best fit to a Boltzmann distribution is also reported for the product. (a)  $n = 50$ ; (b)  $n = 100$ .

strongly depend on cluster size. It is worth comparing the present approach to the results obtained by Stace on  $\text{Ar}_n^+$  clusters.<sup>4</sup> The physical conditions chosen by this author are those of a cold thermal distribution of  $J$ , with an infinitely narrow extra vibrational energy distribution located at  $\Delta E$ . Because  $\Delta E$  is very large in this work (1 eV), many evaporations will occur, and the width of the vibrational energy distribution does not really matter. Hence we can safely take  $T_{\text{vib}} = T_{\text{rot}}$ . We have calculated the ratio  $T_{\text{rot}}^{(f)} / T_{\text{rot}}^{(i)}$  between the final and initial rotational temperatures, for  $\text{LJ}_{50}$  and at several excitation energies in the range  $0 \leq \Delta E \leq 80$  LJ units. The value used by Stace corresponds approximately here to  $\Delta E \sim 50$ –80 units. The results are plotted in Fig. 7. At small extra excitation energies,  $J_c$  is

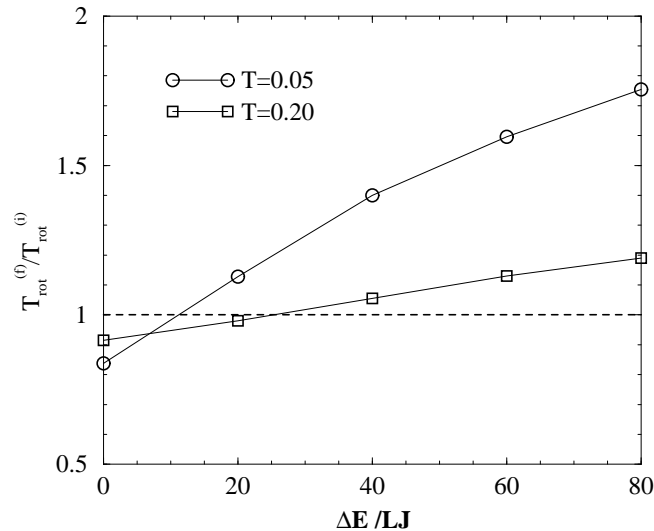


FIG. 7: Final/initial rotational temperature ratio following evaporation of  $\text{LJ}_{51}$ , for two thermal distributions at  $T = 0.05$  and  $T = 0.20$ , as a function of the extra excitation energy.

small and evaporation is more likely accompanied with rotational cooling. On the other hand, at large values of  $\Delta E$ , rotational heating occurs easily. It seems also pretty obvious that the smaller the initial temperature, the stronger the



heating at a given excitation energy. The transition between cooling and heating occurs near  $\Delta E = 12$  (for  $T = 0.05$ ) and  $\Delta E = 25$  (for  $T = 0.20$ ), and we do not find any evidence for rotational cooling in LJ<sub>50</sub> at excitation energies as large as 50 LJ units. This is in clear contradiction with the results by Stace,<sup>4</sup> who found heating after a single evaporation in clusters smaller than 30 atoms, and cooling in 40- and 50-atom clusters at  $T \sim 0.05$ . At  $T \sim 0.20$ , only the 10-atom cluster undergoes rotational heating. This trend is also observed in our work, since an increase in the initial rotational temperature indeed favors cooling.

#### IV. DISCUSSION AND CONCLUSION

Systematic investigations<sup>6,8</sup> have shown that phase space theory, in the sense of Chesnavich and Bowers,<sup>14</sup> performs much better than RRK or Weisskopf-Engelking models in reproducing the data of reference trajectory simulations. Weerasinghe and Amar emphasized that the interaction between an atom and the remaining cluster could not be modelled by a simple  $C/r^n$  potential, and that the geometrical extent of the system had to be taken into account. The detailed studies by Peslherbe and Hase<sup>8</sup> on rotating and nonrotating aluminium clusters confirmed the general agreement between PST and MD, but they noticed some deviations at large excitation energies. Probably the simple form chosen for the dissociation potential is not appropriate for these clusters, for which the interatomic potential (Lennard-Jones pairwise + Axilrod-Teller three-body component) is also not fully isotropic.

To our knowledge, there has not been any attempt at describing evaporation in rotating clusters using PST, except in the works by Peslherbe and Hase.<sup>7,8</sup> One of the interesting results found in the present work concerns the shape of the distribution of the product angular momentum, which was seen to have a discontinuity in its derivative for  $J = J_r$ . The statistics gathered by Peslherbe and Hase [100 trajectories for a given  $(E, J)$ <sup>8</sup>] are probably not sufficient to confirm this prediction, and we see that 15 sets of 5000 trajectories are necessary to get a hint at this effect.

Here, we have used PST in its general form, assuming that both energy and angular momentum were conserved during dissociation, calculating transition state properties at the centrifugal barrier, and without assuming a  $C/r^n$  form for the interaction potential between fragments. The main approximation was to treat the product cluster as a sphere, but this seems appropriate, in practice, for a large cluster in its liquidlike phase.

The significant differences between the present results and the work by Stace<sup>4</sup> probably comes from the assumption made by this author that all translational energies released are uniformly distributed. This is a very strong assumption, which, as a matter of fact, prevents a rigorous conservation of energy during dissociation. Its consequence is that the most probable value of  $\varepsilon_t$  is  $(E - E_0)/2$ , much too large with respect to the simple RRKM estimate given by  $(E - E_0)/s$ . Therefore rotational energies are significantly underestimated, which is precisely observed under the form of preferential cooling. To confirm these differences between our work and the results by Stace, we have performed additional MD simulations of LJ<sub>10</sub>, at the same conditions as above for  $n = 50$ . In particular, we have carefully looked at the distribution of final angular momentum of the product LJ<sub>9</sub>, but we could not find any signature of bimodality, contrary to the picture discussed in Ref. 4. Our PST calculations, within the harmonic and simple potential approximations, show a stronger rotational heating than the Stace prediction: for  $T_{\text{rot}}^{(i)} = 0.05$  we get  $T_{\text{rot}}^{(f)} = 0.28$  at an extra excitation energy  $\Delta E = 25$  units only (in agreement with MD), instead of  $T_{\text{rot}}^{(f)} \approx 0.22$  for  $\Delta E > 50$  units in Stace's work.<sup>4</sup>

Even though the harmonic approximation may be questioned at high energies, it allowed us to undertake quantitative studies for clusters containing an arbitrary number of atoms. This required some elementary properties such as rotational constants or binding energies to be approximated in a liquid drop fashion, with explicit functions of size. Surely this approach is too simplistic, as it neglects non-monotonic finite size effects.<sup>24</sup> The form chosen for the interaction potential may also not be appropriate for very large sizes, for which the location of the centrifugal barrier becomes of the same magnitude as the cluster radius itself. Fortunately the numerical effort involved in the calculations of the anharmonic DOS and the effective dissociation potential is comparatively smaller than running a series of trajectories, especially at low energies where the dissociation rate is vanishingly small.

The work carried out in this paper and in our previous article<sup>5</sup> can be straightforwardly extended to the case of multiple (sequential) evaporations, which arise at large excitation energies, and it should be possible to overcome most of the limitations that Stace had to impose.<sup>4</sup> Possible connections with the search for a liquid-gas transition in finite systems<sup>3,16,18</sup> could then be investigated. Another extension to molecular clusters would also be of great interest, as there are presently only very few available theoretical results based on statistical analyses at the level of phase space theory.

## Acknowledgments

The authors wish to thank the GDR *Agrégats, Dynamique et Réactivité* for financial support.

- 
- <sup>1</sup> C. Bréchignac, Ph. Cahuzac, B. Concina, J. Leygnier, B. Villard, P. Parneix, and Ph. Bréchignac, Chem. Phys. Lett. **335**, 34 (2001).
  - <sup>2</sup> M. Vogel, K. Hansen, A. Herlert, and L. Schweikhard, Phys. Rev. Lett. **87**, 013401 (2001).
  - <sup>3</sup> C. Bréchignac, Ph. Cahuzac, B. Concina, and J. Leygnier, Phys. Rev. Lett. **89**, 203401 (2002).
  - <sup>4</sup> A. J. Stace, J. Chem. Phys. **93**, 6502 (1991).
  - <sup>5</sup> F. Calvo, P. Parneix, J. Chem. Phys. **119**, 256 (2003).
  - <sup>6</sup> S. Weerasinghe, F.G. Amar, Z. Phys. D: At., Mol. Clusters **20**, 167 (1991); J. Chem. Phys. **98**, 4967 (1993).
  - <sup>7</sup> G. H. Peslherbe and W. L. Hase, J. Chem. Phys. **105**, 7432 (1996).
  - <sup>8</sup> G. H. Peslherbe and W. L. Hase, J. Phys. Chem. A **104**, 10556 (2000).
  - <sup>9</sup> P. Pechukas and J. C. Light, J. Chem. Phys. **42**, 3281 (1965).
  - <sup>10</sup> J. C. Light, Discuss. Faraday. Soc. **44**, 14 (1967).
  - <sup>11</sup> C. E. Klotz, J. Phys. Chem. **75**, 1526 (1971).
  - <sup>12</sup> C. E. Klotz, J. Chem. Phys. **64**, 4269 (1976).
  - <sup>13</sup> W. J. Chesnavich and M. T. Bowers, J. Am. Chem. Soc. **98**, 8301 (1976).
  - <sup>14</sup> W. J. Chesnavich and M. T. Bowers, J. Chem. Phys. **66**, 2306 (1977).
  - <sup>15</sup> W. J. Chesnavich and M. T. Bowers, J. Am. Chem. Soc. **99**, 1705 (1977).
  - <sup>16</sup> M. Schmidt, T. Hippler, J. Donger, W. Kronmüller, B. von Issendorff, H. Haberland, and P. Labastie, Phys. Rev. Lett. **87**, 203402 (2001).
  - <sup>17</sup> P. Parneix, F. G. Amar, and Ph. Bréchignac, J. Phys. Chem. **239**, 121 (1998).
  - <sup>18</sup> J. Pochodzalla, T. Möhlenkamp, T. Rubehn *et al.*, Phys. Rev. Lett. **75**, 1040 (1995).
  - <sup>19</sup> F. Calvo and P. Labastie, Euro. Phys. J. D **3**, 229 (1998).
  - <sup>20</sup> M. F. Jarrold, *Introduction to statistical reaction theories*, in Clusters of Atoms and Molecules I, edited by H. Haberland (Springer, Berlin), 1991.
  - <sup>21</sup> R. H. Swendsen and J.-S. Wang, Phys. Rev. Lett. **57**, 2607 (1986); G. J. Geyer, in *Computing Science and Statistics: Proceedings of the 23rd Symposium on the Interface* (American Statistical Association, New York, 1991).
  - <sup>22</sup> A. M. Ferrenberg and R. H. Swendsen, Phys. Rev. Lett. **61**, 2635 (1988).
  - <sup>23</sup> One angular momentum LJ unit equals  $33.41\hbar$  for Argon.
  - <sup>24</sup> J. Jortner, Z. Phys. D: At., Mol. Clusters **24**, 247 (1992).